ELSEVIER

NeuroImage

www.elsevier.com/locate/ynimg
NeuroImage 32 (2006) 1113 – 1119

Technical Note

Automated Brainstem Co-registration (ABC) for MRI

Vitaly Napadow,[a,*] Rupali Dhond,[a] David Kennedy,[b] Kathleen K.S. Hui,[a] and Nikos Makris[b]

[a]*Martinos Center for Biomedical Imaging, Department of Radiology, Massachusetts General Hospital, Charlestown, MA, USA*
[b]*Center for Morphometric Analysis, Department of Neurology, Massachusetts General Hospital, Charlestown, MA, USA*

Received 4 February 2006; revised 11 May 2006; accepted 23 May 2006
Available online 12 July 2006

Group data analysis in brainstem neuroimaging is predicated on accurate co-registration of anatomy. As the brainstem is comprised of many functionally heterogeneous nuclei densely situated adjacent to one another, relatively small errors in co-registration can manifest in increased variance or decreased sensitivity (or significance) in detecting activations. We have devised a 2-stage automated, reference mask guided registration technique (Automated Brainstem Co-registration, or ABC) for improved brainstem co-registration. Our approach utilized a brainstem mask dataset to weight an automated co-registration cost function. Our method was validated through measurement of RMS error at 12 manually defined landmarks. These landmarks were also used as guides for a secondary manual co-registration option, intended for outlier individuals that may not adequately co-register with our automated method. Our methodology was tested on 10 healthy human subjects and compared to traditional co-registration techniques (Talairach transform and automated affine transform to the MNI-152 template). We found that ABC had a significantly lower mean RMS error (1.22 ± 0.39 mm) than Talairach transform (2.88 ± 1.22 mm, $\mu \pm \sigma$) and the global affine (3.26 ± 0.81 mm) method. Improved accuracy was also found for our manual-landmark-guided option (1.51 ± 0.43 mm). Visualizing individual brainstem borders demonstrated more consistent and uniform overlap for ABC compared to traditional global co-registration techniques. Improved robustness (lower susceptibility to outliers) was demonstrated with ABC through lower inter-subject RMS error variance compared with traditional co-registration methods. The use of easily available and validated tools (AFNI and FSL) for this method should ease adoption by other investigators interested in brainstem data group analysis.

Keywords: Functional MRI; Tractography; Talairach and Tournoux; Alignment

Introduction

In neuroimaging, group analysis of functional and structural data from multiple individuals is predicated on accurate co-registration of anatomy. Without adequate registration, functional activity or structural parameters that have been assigned to a known region in one individual cannot be compared or averaged with data from the same coordinate in another individual. While validated automated methods exist for cortical and subcortical registration (Friston et al., 1995; Fischl et al., 1999b; Jenkinson et al., 2002), these methods have not been tested for brainstem-specific analyses.

Typically, co-registration has been done with either manual or automated registration techniques. Automated registration, which calculates a transformation matrix based on an optimization of some global measure of similarity between two images, has the advantage of minimizing user interface time and subjectivity. However, the calculated transform solves a global optimization problem and may not be accurate for specific sub-regions of the brain. On the other hand, manual techniques utilize user-defined markers that are unique and are consistently located within individual subjects' anatomical brain images. Once a common set of landmarks has been defined on each individual brain, an affine transformation is computed which minimizes the error between landmarks. Advantages of this technique include simplicity and speed in calculating the transform, as well as excellent alignment near the chosen landmarks. Disadvantages of manual registration include a requirement for training in landmark selection, the time-consuming nature of manual editing, and the somewhat subjective nature of landmark definition. Furthermore, while alignment may be excellent near chosen landmarks, accuracy typically falls off with distance away from these landmarks. For example, cortical and brainstem co-registration is suboptimal with the stereotactic atlas methods of Talairach and Tournoux, which utilize 8 reference landmarks (Talairach and Tournoux, 1988).

Structural and functional studies of brainstem data have typically taken four different approaches to group analysis. Several studies have linearly transformed functional MRI (fMRI) data to the landmark-based Talairach and Tournoux coordinate system before deriving group brainstem activation maps (DaSilva et al., 2002; Zhang et al., in press). Other fMRI studies have instead used

* Corresponding author. 149, 13th St. Rm. 2301, Charlestown, MA 02119, USA. Fax: +1 617 726 7422.
E-mail address: vitaly@nmr.mgh.harvard.edu (V. Napadow).
Available online on ScienceDirect (www.sciencedirect.com).

1053-8119/$ - see front matter © 2006 Elsevier Inc. All rights reserved.
doi:10.1016/j.neuroimage.2006.05.050

automated linear (affine) transformation to an atlas template prior to deriving fMRI group brainstem maps (McKay et al., 2003; Dunckley et al., 2005; Zambreanu et al., 2005). However, many investigators, recognizing the current suboptimal approaches to brainstem co-registration, have instead opted for individual-space ROI approaches (Guimaraes et al., 1998; Komisaruk et al., 2002; Tracey et al., 2002; Liu et al., 2004; Topolovec et al., 2004; Hawley et al., 2005). Individual-based approaches have also been typical in studies of brainstem structure with DTI and tractography (Fitzek et al., 2001; Stieltjes et al., 2001; Nagae-Poetscher et al., 2004; Salamon et al., 2005).

A fourth approach involves nonlinear co-registration through elasticity, fluid, and demon co-registration algorithms (Christensen et al., 1994; Thirion, 1998; Ashburner and Friston, 1999). While these methods can be plagued by high dimensionality leading to excessively lengthy computation time, they provide a means for higher precision in registering complex 3D shapes. A semi-automated nonlinear approach has been developed for localization of brainstem lesions and involves the nonlinear warping of a structural dataset to a normalized stereotactic-atlas-based brainstem model (Capozza et al., 2000; Cruccu et al., 2005). While this method has been successfully applied to correlate specific brainstem lesions with various neurophysiological and clinical findings (Cruccu et al., 2005), it works on the high resolution anatomical data itself, and it remains to be seen if deformation fields derived by this method could successfully warp low-resolution fMRI or diffusion-weighted data affected by susceptibility artifact. Furthermore, the amount of manual intervention necessary in this method may be prohibitive for wider adoption.

In this report, we present the Automated Brainstem Co-registration (ABC) method, which combines a globally derived affine transformation followed by a brainstem-weighted second affine transform stage. Our method also contains an option for manual co-registration in cases of individual outliers. The first ABC stage utilizes automated registration with a previously validated methodology (FLIRT, FSL). The second stage performs automated registration with the aid of a reference-weighted volume focused on the brainstem. Alternatively, our manual-landmark-based option follows the automated first stage with manually defining 12 landmarks and performing an affine transformation to minimize errors between landmarks. Both ABC and the semi-automated option were found to have significant advantages in brainstem co-registration over traditional whole-brain registration approaches.

Overview and evaluation of methodology

Subjects and scan parameters

Our methods were developed and tested on a group of ten (10) anatomical datasets collected from healthy adult subjects (4 M, 6F, 21–32 years old). All participants in the study provided written informed consent in accordance with the Human Research Committee of the Massachusetts General Hospital.

MRI was performed on a 3 T Siemens Trio scanner equipped with an 8-channel head coil. For each individual, two T1-weighted structural MRI scans were acquired with a three-dimensional magnetization-prepared rapid acquisition gradient echo (3D-MPRAGE) pulse sequence (TR/TE = 2530/3.36 ms; FOV = 256 mm; F.A. = 7°; TI = 1100 ms; spatial resolution = 1.0 × 1.0 × 1.3 mm). These two structural scans were normalized, co-registered, and averaged following the methods outlined in our center with the Freesurfer data processing package (Dale et al., 1999; Fischl et al., 1999a). These data were then subjected to ABC, which is a two-stage process of co-registration.

Automated global first stage

The first stage in the inter-subject co-registration process involved global automated co-registration of skull-stripped anatomical datasets to the MNI-152 template (Collins et al., 1994) using affine transformation. An affine transformation preserves collinearity and is typically composed of rotations, translations, dilations, and shears. This first stage provides a globally adequate co-registration that can be used without stage 2 (reference volume optimization or manual landmarks) for group analysis outside of the brainstem, as well as an excellent starting point for stage 2. To accomplish this first stage, we utilized an existing proven algorithm for both skull stripping (Brain Extraction Tool, BET, FSL, (Smith, 2002) and affine co-registration (FMRIB's Linear Image Registration Tool, FLIRT, FSL; Jenkinson et al., 2002). FLIRT was run using the correlation ratio cost function, tri-linear interpolation, and 12 degrees of freedom (full set affine transformation).

Automated-brainstem-weighted second stage

The ABC method follows the first stage global co-registration with a second brainstem-weighted affine transformation. To accomplish improved brainstem co-registration, we created a mask of the MNI-152 brainstem that included surrounding low-intensity cerebral–spinal fluid (CSF) voxels (Fig. 1). Voxels inside the mask were set to 1, while voxels outside the mask were set to 0. This mask was used as a reference volume to weight the correlation ratio cost function in FLIRT. Weighting reflects the importance of regions to successful co-registration, and this mask was created on the template (as opposed to individual brains) for uniformity and in order to save manual intervention time in future brainstem co-registrations. Cost function weighting is typically used to down-weight artifactual and pathological brain regions in order to keep them from disrupting automated co-registration. In our case, we used the reference volume to focus co-registration on a specific region of interest—the brainstem. Once our brainstem mask weighting volume was created, it was used in a second co-registration stage which incorporated a full affine transform using FLIRT and the correlation ratio cost function. Conversely, this methodology can also be implemented within other fMRI software packages, such as AFNI and SPM, which incorporate cost function weighting volumes for automated co-registration.

Landmark definitions for manual outlier co-registration option and validation

For cases of individual brainstem outliers that may not co-register correctly with ABC, the second stage can alternatively incorporate Landmark-guided Brainstem Co-registration (LBC) through a set of 12 landmarks around the brainstem. These landmarks were also used to help validate the ABC method. They were chosen at high-contrast boundaries, in areas of high curvature (in order to limit user error due to landmark ambiguity), and around important brainstem functional centers (as registration is most improved in proximity to landmarks). The number of landmarks (12) has been limited from a larger number in order to

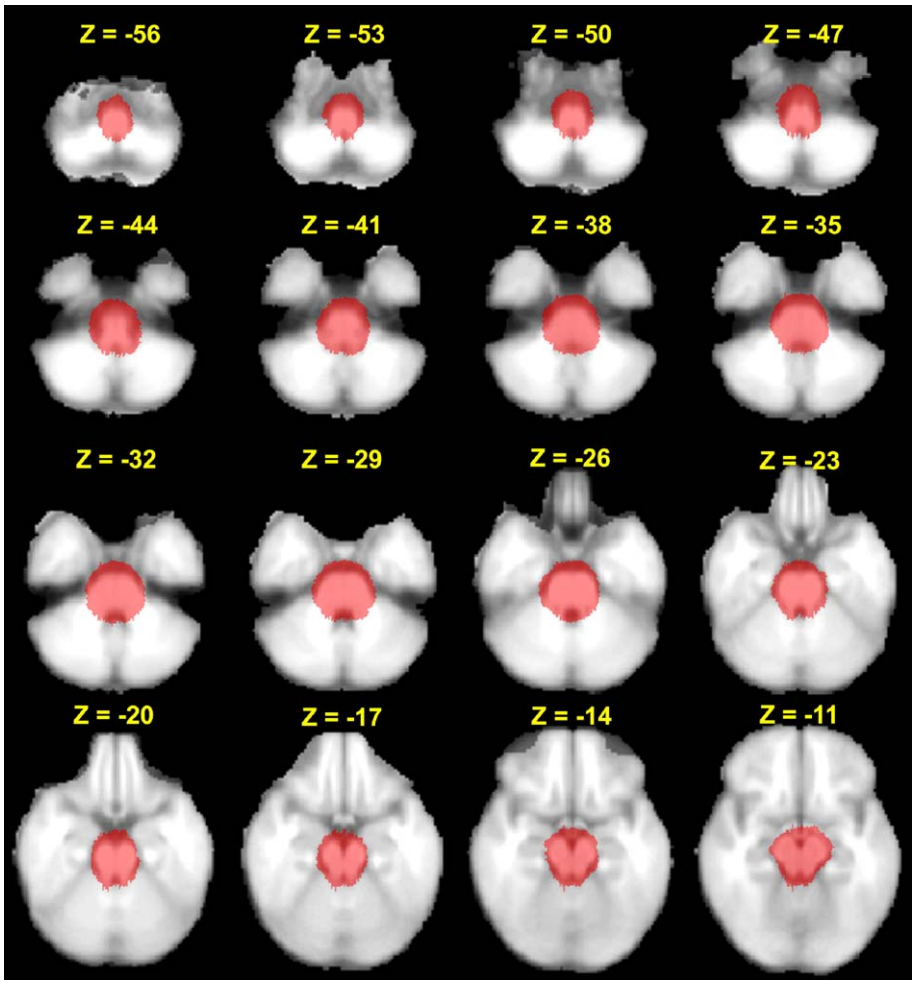

Fig. 1. For Automated Brainstem Co-registration (ABC), a mask volume dataset was created which incorporated the brainstem and surrounding CSF. This dataset was used to weight the cost function in a second stage affine co-registration.

minimize user intervention time while still capturing the main sources of structural variability in the brainstem. Conversely, while fewer landmarks may also have improved co-registration, the potential of mis-registering an anatomical outlier (one not included in our sample) by using too few landmarks may be more deleterious than the benefit gained from slightly reduced user interaction time. The first eight landmarks were defined in the mid-sagittal plane, while the final four landmarks delimited brainstem medial–lateral thickness at the pontine and medullary levels. The twelve (12) landmark tags and the best orientation for localization are defined below (see also Fig. 2):

1. [sagittal] anterior commissure
2. [sagittal] posterior commissure
3. [sagittal] ventral pontomesencephalic notch/interpeduncular fossa
4. [sagittal] ventral median fissure at pontomedullary notch
5. [sagittal] obex
6. [sagittal] inferior limit of Aqueduct of Sylvius/anterior medullary velum
7. [sagittal] ventral border of pons, axial level with trigeminal n. (CN V)
8. [sagittal] dorsal border of pons, axial level with CN V
9. [coronal] right lateral border of pons, axial level with CN V, coronal level with the tag 7/tag 8 midpoint
10. [coronal] left lateral border of pons, axial level with CN V, coronal level with the tag 7/tag 8 midpoint
11. [coronal] right lateral border of medulla, axial and coronal level with the tag 4/tag 5 midpoint
12. [coronal] left lateral border of medulla, axial and coronal level with the tag 4/tag 5 midpoint

It should be noted that, in order to define tags 7 through 10, the user must locate the axial plane containing the trigeminal nerve (CN V). This nerve, a high intensity structure on T1-weighted images, is best found on coronal slices just lateral to the lateral border of the pons (Fig. 2, see Haines, 1991 for anatomical references). If the roots of CN V are not in the same axial plane, the axial plane was chosen to be equidistant from the left and right root centers. Total interaction time for an experienced user was found to be less than 10 min per brainstem.

Tag definition and the optimal affine transform calculation were completed using a least squares algorithm from already existing and validated software (3dTagalign, AFNI, Cox, 1996). Individual tagged datasets were aligned to a tagged version of the same

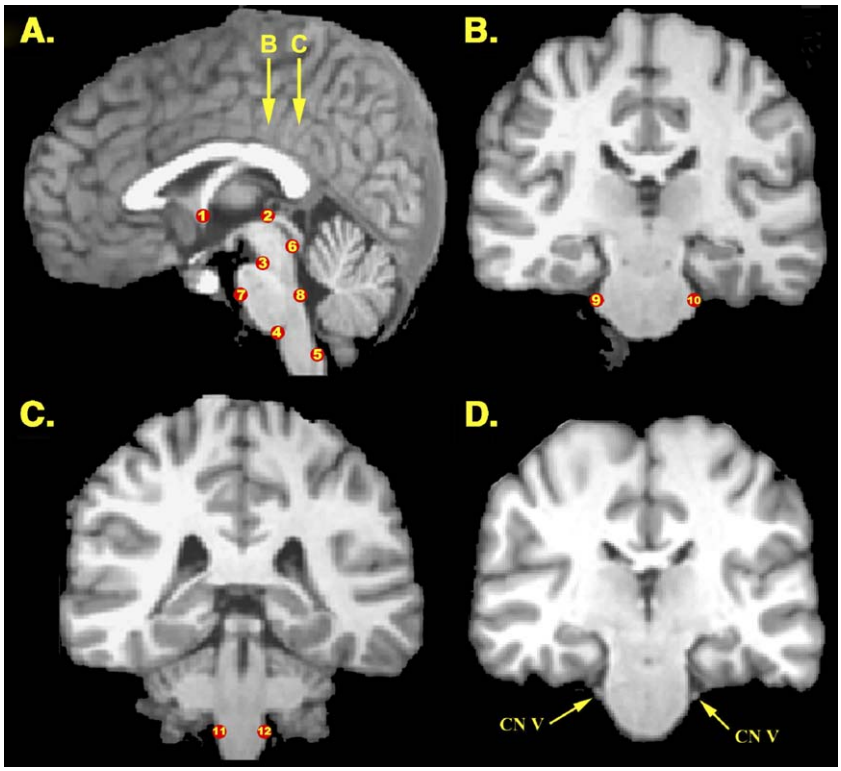

Fig. 2. (A) For Landmark-guided Brainstem Co-registration (LBC), the majority of landmarks were defined in the mid-sagittal plane of a dataset previously aligned to the MNI-152 template through an automated algorithm. (B) Landmarks 9 and 10 are found in a coronal slice located midway between landmarks 7 and 8. (C) Landmarks 11 and 12 are found in a coronal slice located midway between landmarks 4 and 5. (D) Landmarks 7 and 8 are located based on the axial plane location of the trigeminal nerve (CN V).

template used for automated co-registration—the 152 brain MNI atlas.

In order to validate the ABC method and to compare our method with more traditional methods, the root-mean-square (RMS) error from the tagged MNI-152 atlas was computed for the 12 landmarks for ABC and LBC, as well as traditional co-registration techniques (see below).

Comparison to traditional methods

For comparison purposes, in addition to the conventional global affine-to-MNI first stage (above), a separate analysis was completed wherein all brains were transformed to classical Talairach space (Talairach and Tournoux, 1988) as this group analysis normalization method has also been used by fMRI data analysis software (e.g. AFNI). Talairach transformation was also completed for the MNI-152 template (as these atlases are slightly different).

Accuracy

In order to quantify accuracy, RMS error calculations for all four methods (Talairach transformation, global affine-to-MNI transformation, ABC, and LBC) were compared with a pairwise Student's t test, significant at $P < 0.05$ adjusted for multiple comparisons. We found that the RMS error for the Talairach (2.88 ± 1.22 mm, $\mu \pm \sigma$) and global affine methods (3.26 ± 0.81 mm) were significantly greater than in ABC (1.22 ± 0.39 mm, at $P < 0.01$ and $P < 1 \times 10^{-6}$, respectively) and LBC (1.51 ± 0.43 mm, at $P < 0.05$ and $P < 1 \times 10^{-4}$, respectively, Fig. 3). No significant difference was found between ABC and LBC ($P = 0.191$). Accuracy was also judged qualitatively for all four methods by deriving a 10-subject average brain and visualizing individual brainstem borders onto this average (Fig. 4). Visualization was done in the mid-sagittal plane as this orientation accentuates the source for greatest anatomical variance—the angle subtended by the brainstem longitudinal axis from the AC–PC plane. By defining the longitudinal brainstem axis by a least squares fit line through tags 5, 6, and 8, the angle subtended was found to range from 71.4° to 79.6° using the global affine method, 72.1° to 78.3° using the Talairach transform method, 73.0° to 76.6° using ABC, and 71.1° to 79.5° using LBC. The inferior border for individual outlines was defined by the axial plane containing the obex. Qualitatively, the brainstem outlines for ABC and LBC both demonstrated more consistent and uniform overlap than for the Talairach or global affine methods.

Robustness

In order to quantify robustness (lower susceptibility to outliers), inter-subject variances from each method were compared with an F test, significant at $P < 0.05$. The RMS error variance with ABC (0.16 mm^2) was lower than the variance in Talairach transformation (1.49 mm^2, $P < 0.005$) and was lower than the global affine method (0.66 mm^2, $P < 0.05$). We also found that the RMS error variance with LBC (0.18 mm^2) was lower than the variance in Talairach transformation ($P = 0.005$) and was trending lower compared to the global affine method ($P = 0.07$).

Quantifying RMS error for different landmarks across individuals defines where localization variability arises. This analysis

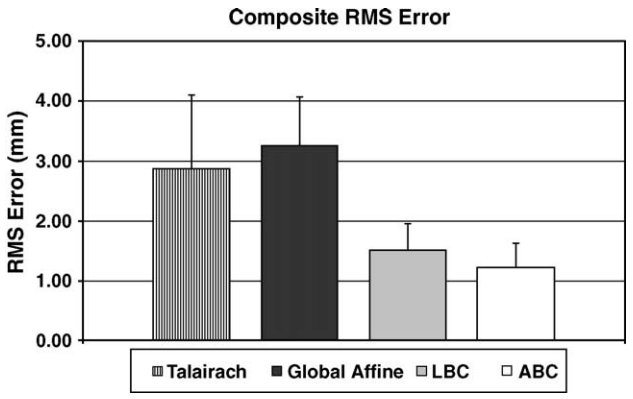

Fig. 3. Brainstem co-registration accuracy for Talairach, global affine, LBC, and ABC methods was assessed by mean RMS error from a tagged version of the MNI-152 template. ABC and LBC produced less RMS error than the traditional methods.

was done for all four methods (Fig. 5), and tag-specific RMS errors were compared with pairwise Students' *t* tests, corrected for multiple comparisons. For the Talairach method, tags 11 (3.55 ± 2.24 mm) and 12 (3.49 ± 2.20 mm) had the greatest RMS errors, and these errors were statistically greater than for tag 2 (0.40 ± 0.52 mm). For the global affine method, tags 5 (4.36 ± 1.84 mm) and 12 (3.84 ± 1.58 mm) were found to have the greatest RMS errors from template and were statistically greater than tag 2 (1.93 ± 0.65 mm, $P < 0.05$). For neither ABC nor LBC did RMS error vary significantly across tags. In summary, for the Talairach and affine-to-MNI methods, the most error-prone tags were the most inferior (tags 5, 11 and 12), while tag 2 (posterior commissure) was the least error-prone and is, in fact, one of the cardinal landmarks of the Talairach method (Talairach and Tournoux, 1988). Furthermore, individual tag RMS error with ABC and LBC was significantly less than the affine-to-MNI method ($P < 0.05$) for all tags except tags 2, 7, and 8.

It should be noted that the affine transforms derived by ABC must be applied to any functional or structural data that are to be passed up to a higher level group analysis. In applying our method to functional brainstem data, we recommend concatenating the two affine transformation matrices derived in stage 1 (global affine) and stage 2 (reference volume weighted or landmark-guided affine transform) into a single affine transformation matrix. Applying this combined transform in a single step will limit interpolation errors, which may compound in a multi-stage process.

Discussion

Incorporating functional and structural brain data in a group analyses with different subjects is problematic due to inherent individual variability in brainstem orientation and volume. While current methods for inter-subject anatomical brain co-registration may not adequately co-register the brainstem, our method provides a brainstem focused addendum which significantly improves both the accuracy and robustness of co-registration. We have developed our methods on a platform of previously validated and easily available software packages, namely AFNI and FSL (Cox, 1996; Jenkinson et al., 2002), in order to simplify adoption by other investigators.

Our results demonstrate that ABC improved both accuracy and robustness of anatomical inter-subject co-registration for the brainstem. Accuracy was assessed by both qualitative and quantitative means. Post-registration brainstem contours in the mid-sagittal plane demonstrated clearly improved overlap with our methods compared to the conventional Talairach and global affine approaches. This overlap was quantified by deriving the RMS error between landmarks placed on individuals to the same landmarks placed on a canonical brain template (MNI-152 brain atlas). The

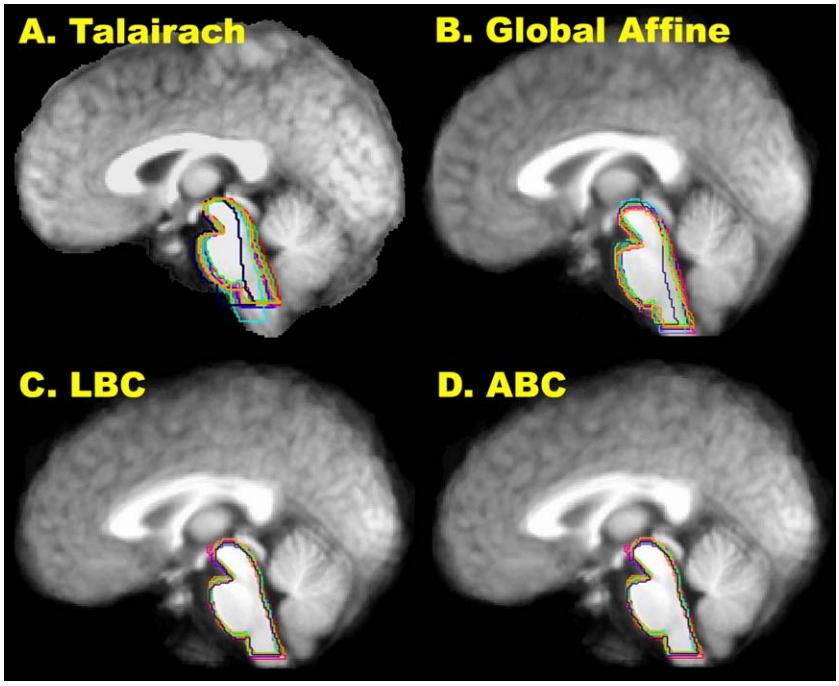

Fig. 4. The outlines of individual brainstems in the mid-sagittal slice are visualized onto a group-averaged structural dataset. Individual brainstems were co-registered by (A) Talairach transform, (B) global affine transform, (C) LBC, and (D) ABC.

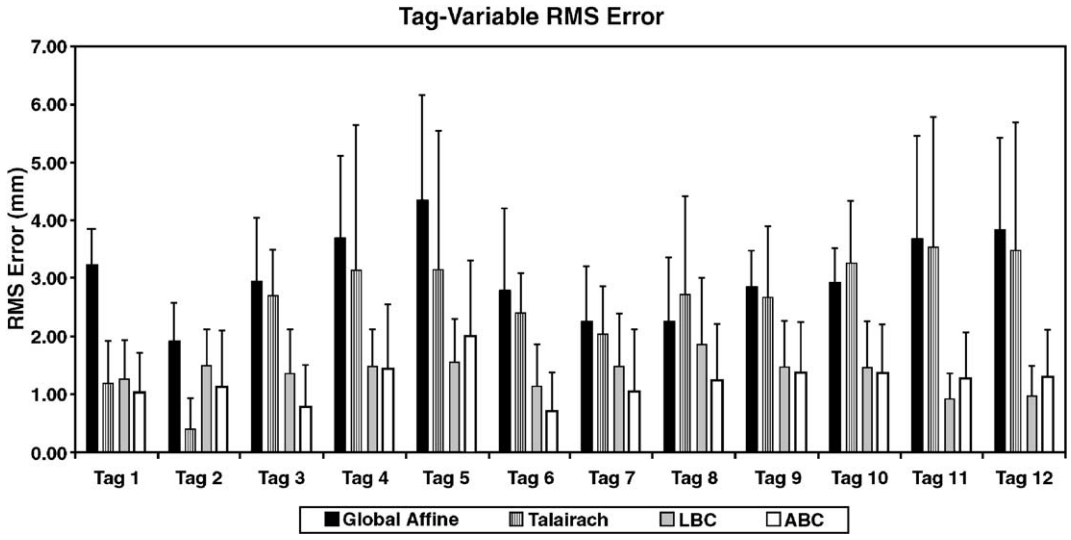

Fig. 5. The traditional Talairach transform and global affine methods lead to variable RMS error for different tags, whereas RMS error was more homogeneous with our ABC and LBC methods. Individual tag variability was assessed by tag-specific RMS error and demonstrated that mis-registration was worse in tags located furthest from the midbrain tegmentum for the two traditional methods. In addition, individual tag RMS error with ABC and LBC was significantly less than the global affine method for all tags except tags 2, 7, and 8.

mean RMS errors for the Talairach and global affine methods were 2.88 mm and 3.26 mm, respectively. These errors are on the order of functional MRI voxel size in typical fMRI studies. In contrast, our ABC method produced a mean tag RMS error of 1.22 mm (1.51 mm with the LBC option), which is on the order of voxel size in "high-resolution" fMRI studies. Empirically, some investigators have suggested that optimal voxel size for reliable activation in the brainstem is ~3 mm (Dunckley et al., 2005), which may be at or below the potential inter-subject anatomical co-registration error.

Thus, the improved accuracy described by our method would represent not only a theoretical improvement, but also a practical improvement for functional MRI studies of brainstem activation. For example, the mean RMS errors quantified from the Talairach and global affine co-registration methods may lead to misinterpretations in assigning functional activity to specific brainstem nuclei. Errors in the anterior–posterior dimension could lead to assignment of functional activity to more ventrally located structures such as the inferior olivary nucleus instead of more dorsally located nucleus ambiguous or reticular nuclei in the medulla. Similarly, errors in the cranial–caudal dimension could lead to misattribution of functional activity to the substantia nigra instead of the more ventrally located pontine nuclei, or vice versa. Errors in the medial–lateral dimension could lead to assignment of functional activity to the midline raphe nuclei instead of the more laterally located reticular nuclei. As the brainstem is comprised of many functionally heterogeneous nuclei densely situated adjacent to one another, relatively small errors in localization can lead to large misinterpretations of functional significance.

Furthermore, the robustness of ABC was shown to be superior to conventional methods by statistically comparing variance in RMS error with an F test. Individual anatomical outliers would produce higher landmark RMS errors and contribute to a greater variance. Both ABC and LBC demonstrated lower variance in RMS error compared with the conventional methods. Individual outliers were also easily visualized by the brainstem border outlines (e.g. dark and light blue outlines). These outliers may significantly skew group results if they are not co-registered with other subjects, especially if they represent not only anatomical outliers, but functional activation outliers as well. Furthermore, the degree to which an individual brainstem is a structural outlier may define the choice between ABC and LBC. We suggest that ABC be utilized as the typical brainstem co-registration method. Upon evaluation of goodness of fit, if co-registration is judged to be suboptimal, then our manual-landmark-based method (LBC) should be adopted. LBC may be less sensitive to a successful 1st stage co-registration, while ABC may be dependent on the template-based brainstem mask volume approximating the location of the individual subject brainstem after the 1st automated stage.

In assessing the traditional methods for anatomical co-registration, accuracy decreased with caudal distance away from the midbrain tegmentum. This is to be expected for the Talairach method, where accuracy is best in proximity with the cardinal landmarks (anterior and posterior commissures). Furthermore, brainstem anatomy is highly variable in the sagittal plane in the angle subtended by the brainstem longitudinal axis from the AC–PC line. Thus, the error from any template should increase roughly as $r\alpha$, where r is the distance along this longitudinal axis and α is the angular error from the template longitudinal axis. For LBC, RMS error did not vary significantly across tags, as would be expected for a method that adopts a least squares approach to minimize tag error. In a direct comparison, individual tag RMS error for both ABC and LBC was significantly lower than the global affine method for all tags except tags 2, 7, and 8. Tag 2 is the posterior commissure, which was the best aligned tag for the global affine method. Tags 7 and 8, which define the ventral and dorsal edge of the pons, were also already well aligned by this method, thus the improvement with ABC or LBC did not reach statistical significance for these tags.

It should also be noted that other factors may also add artifactual variability to brainstem-specific group analyses. For example, co-registration of individual lower resolution functional or diffusion-weighted data to their high resolution anatomical dataset may also be suboptimal. This problem is particularly exacerbated by susceptibility-artifact-induced signal loss along the

anterior edge of the pons. Future efforts should also address this important source of error, which can lead to misattribution of functional activity and white matter structure in the individual and corrupt group averaging analyses.

We have demonstrated a fully automated, two-stage brainstem co-registration method for improved inter-subject brainstem alignment. Our methodology was shown to be not only more accurate than traditional whole-brain approaches, but could also adequately co-register structural outliers. The use of easily available and validated tools (AFNI and FSL) for our method should ease adoption by other investigators interested in brainstem data group analysis.

Acknowledgments

We would like to thank NCCAM, NIH for funding support for the accomplishment of this project (K01-AT002166-01, P01-AT002048-02), as well the NCRR (P41RR14075) and the Mental Illness and Neuroscience Discovery (MIND) Institute.

References

Ashburner, J., Friston, K.J., 1999. Nonlinear spatial normalization using basis functions. Hum. Brain Mapp. 7 (4), 254–266.

Capozza, M., Iannetti, G.D., Mostarda, M., Cruccu, G., Accornero, N., 2000. Three-dimensional mapping of brainstem functional lesions. Med. Biol. Eng. Comput. 38 (6), 639–644.

Christensen, G.E., Rabbitt, R.D., Miller, M.I., 1994. 3D brain mapping using a deformable neuroanatomy. Phys. Med. Biol. 39 (3), 609–618.

Collins, D.L., Neelin, P., Peters, T.M., Evans, A.C., 1999. Automatic 3D intersubject registration of MR volumetric data in standardized Talairach space. J. Comput. Assist. Tomogr. 18 (2), 192–205.

Cox, R.W., 1996. AFNI: software for analysis and visualization of functional magnetic resonance neuroimages. Comput. Biomed. Res. 29 (3), 162–173.

Cruccu, G., Iannetti, G.D., Marx, J.J., Thoemke, F., Truini, A., Fitzek, S., Galeotti, F., Urban, P.P., Romaniello, A., Stoeter, P., Manfredi, M., Hopf, H.C., 2005. Brainstem reflex circuits revisited. Brain 128 (Pt. 2), 386–394.

Dale, A.M., Fischl, B., Sereno, M.I., 1999. Cortical surface-based analysis. I. Segmentation and surface reconstruction. NeuroImage 9 (2), 179–194.

DaSilva, A.F., Becerra, L., Makris, N., Strassman, A.M., Gonzalez, R.G., Geatrakis, N., Borsook, D., 2002. Somatotopic activation in the human trigeminal pain pathway. J. Neurosci. 22 (18), 8183–8192.

Dunckley, P., Wise, R.G., Fairhurst, M., Hobden, P., Aziz, Q., Chang, L., Tracey, I., 2005. A comparison of visceral and somatic pain processing in the human brainstem using functional magnetic resonance imaging. J. Neurosci. 25 (32), 7333–7341.

Fischl, B., Sereno, M.I., Dale, A.M., 1999a. Cortical surface-based analysis: II. Inflation, flattening, and a surface-based coordinate system. NeuroImage 9 (2), 195–207.

Fischl, B., Sereno, M.I., Tootell, R.B., Dale, A.M., 1999b. High-resolution intersubject averaging and a coordinate system for the cortical surface. Hum. Brain Mapp. 8 (4), 272–284.

Fitzek, C., Weissmann, M., Speckter, H., Fitzek, S., Hopf, H.C., Schulte, E., Stoeter, P., 2001. Anatomy of brain-stem white-matter tracts shown by diffusion-weighted imaging. Neuroradiology 43 (11), 953–960.

Friston, K., Ashburner, J., Frith, C.D., Poline, J.-B., Heather, J.D., Frackowiak, R.S.J., 1995. Spatial registration and normalization of images. Hum. Brain Mapp. 2, 165–189.

Guimaraes, A.R., Melcher, J.R., Talavage, T.M., Baker, J.R., Ledden, P., Rosen, B.R., Kiang, N.Y., Fullerton, B.C., Weisskoff, R.M., 1998. Imaging subcortical auditory activity in humans. Hum. Brain Mapp. 6 (1), 33–41.

Haines, D., 1991. Neuroanatomy. Williams and Wilkins, Baltimore.

Hawley, M.L., Melcher, J.R., Fullerton, B.C., 2005. Effects of sound bandwidth on fMRI activation in human auditory brainstem nuclei. Hear. Res. 204 (1–2), 101–110.

Jenkinson, M., Bannister, P., Brady, M., Smith, S., 2002. Improved optimization for the robust and accurate linear registration and motion correction of brain images. NeuroImage 17 (2), 825–841.

Komisaruk, B.R., Mosier, K.M., Liu, W.C., Criminale, C., Zaborszky, L., Whipple, B., Kalnin, A., 2002. Functional localization of brainstem and cervical spinal cord nuclei in humans with fMRI. Am. J. Neuroradiol. 23 (4), 609–617.

Liu, W.C., Feldman, S.C., Cook, D.B., Hung, D.L., Xu, T., Kalnin, A.J., Komisaruk, B.R., 2004. fMRI study of acupuncture-induced periaqueductal gray activity in humans. NeuroReport 15 (12), 1937–1940.

McKay, L.C., Evans, K.C., Frackowiak, R.S., Corfield, D.R., 2003. Neural correlates of voluntary breathing in humans. J. Appl. Physiol. 95 (3), 1170–1178.

Nagae-Poetscher, L.M., Jiang, H., Wakana, S., Golay, X., vanZijl, P.C., Mori, S., 2004. High-resolution diffusion tensor imaging of the brain stem at 3 T. Am. J. Neuroradiol. 25 (8), 1325–1330.

Salamon, N., Sicotte, N., Alger, J., Shattuck, D., Perlman, S., Sinha, U., Schultze-Haakh, H., Salamon, G., 2005. Analysis of the brain-stem white-matter tracts with diffusion tensor imaging. Neuroradiology.

Smith, S.M., 2002. Fast robust automated brain extraction. Hum. Brain Mapp. 17 (3), 143–155.

Stieltjes, B., Kaufmann, W.E., van Zijl, P.C., Fredericksen, K., Pearlson, G.D., Solaiyappan, M., Mori, S., 2001. Diffusion tensor imaging and axonal tracking in the human brainstem. NeuroImage 14 (3), 723–735.

Talairach, J., Tournoux, P., 1988. Co-Planar Stereotactic Atlas of the Human Brain. Thieme, Stuttgart/New York.

Thirion, J.P., 1998. Image matching as a diffusion process: an analogy with Maxwell's demons. Med. Image Anal. 2 (3), 243–260.

Topolovec, J.C., Gati, J.S., Menon, R.S., Shoemaker, J.K., Cechetto, D.F., 2004. Human cardiovascular and gustatory brainstem sites observed by functional magnetic resonance imaging. J. Comp. Neurol. 471 (4), 446–461.

Tracey, I., Ploghaus, A., Gati, J.S., Clare, S., Smith, S., Menon, R.S., Matthews, P.M., 2002. Imaging attentional modulation of pain in the periaqueductal gray in humans. J. Neurosci. 22 (7), 2748–2752.

Zambreanu, L., Wise, R.G., Brooks, J.C., Iannetti, G.D., Tracey, I., 2005. A role for the brainstem in central sensitisation in humans. Evidence from functional magnetic resonance imaging. Pain 114 (3), 397–407.

Zhang, W., Mainero, C., Kumar, A., Wiggins, C., Kwong, K., Benner, T., Purdon, P., Bolar, D., Sorensen, A., in press. Strategies for improving the detection of fMRI activation in trigeminal pathways with cardiac gating. NeuroImage.